Journal of Hazardous Materials 321 (2017) 37–46

Contents lists available at ScienceDirect

Journal of Hazardous Materials

journal homepage: www.elsevier.com/locate/jhazmat

Toxicity mechanisms and synergies of silver nanoparticles in 2,4-dichlorophenol degradation by *Phanerochaete chrysosporium*

Zhenzhen Huang[a,b], Guiqiu Chen[a,b,*], Guangming Zeng[a,b,*], Zhi Guo[a,b], Kai He[a,b], Liang Hu[a,b], Jing Wu[a,b], Lihua Zhang[a,b], Yuan Zhu[a,b], Zhongxian Song[c]

[a] College of Environmental Science and Engineering, Hunan University, Changsha 410082, PR China
[b] Key Laboratory of Environmental Biology and Pollution Control (Hunan University), Ministry of Education, Changsha 410082, PR China
[c] Faculty of Environmental Science and Engineering, Kunming University of Science and Technology, Kunming 650500, PR China

HIGHLIGHTS

- Synergies of AgNPs at low doses (0–60 μM) in 2,4-DCP biodegradation were observed.
- Maximum degradation rates of 2,4-DCP were more than 94% at low-level AgNPs.
- AgNPs-mediated toxicity to *P. chrysosporium* arised from the "Trojan-horse" effects.
- 2,4-DCP was completely degraded into CO_2 and H_2O at optimum conditions.
- Amino, carboxyl, carbonyl and sulfur-containing groups assist in Ag transportation.

GRAPHICAL ABSTRACT

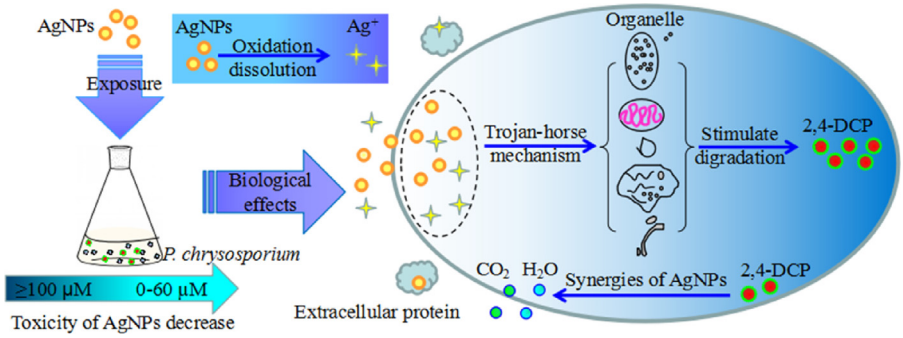

ARTICLE INFO

Article history:
Received 1 July 2016
Received in revised form 29 August 2016
Accepted 30 August 2016
Available online 31 August 2016

Keywords:
Silver nanoparticles
2,4-Dichlorophenol
Phanerochaete chrysosporium
Synergies
Biodegradation

ABSTRACT

Mechanisms of silver nanoparticles-mediated toxicity to *Phanerochaete chrysosporium* and the influence of silver nanoparticles (AgNPs) on the biodegradation of 2,4-dichlorophenol (2,4-DCP) have been systematically investigated. AgNPs at low doses (0–60 μM) have greatly enhanced the degradation ability of *P. chrysosporium* to 2,4-DCP with the maximum degradation rates of more than 94%, exhibiting excellent synergies between AgNPs and *P. chrysosporium* in the degradation of 2,4-DCP. Meanwhile, removal of total Ag was also at high levels and highly pH dependent. However, significant inhibition was highlighted on 2,4-DCP biodegradation and Ag removal upon treatment with AgNPs at high doses and $AgNO_3$ at low-level exposure. Results also suggested that AgNPs-induced cytotoxicity could arise from the "Trojan-horse" mechanism executing particle effects, ion effects, or both, ruling out extracellularly

* Corresponding authors at: College of Environmental Science and Engineering, Hunan University, Changsha 410082, PR China
E-mail addresses: gqchen@hnu.edu.cn (G. Chen), zgming@hnu.edu.cn (G. Zeng).

http://dx.doi.org/10.1016/j.jhazmat.2016.08.075

released Ag^+. Moreover, under relatively low concentrations of AgNPs exposure, 2,4-DCP was broken into linear chain organics, and eventually turned into CO_2 and H_2O through reductive dechlorination and reaction with hydroxyl radicals. FTIR analysis showed that amino, carboxyl, carbonyl, and sulfur-containing functional groups played crucial roles in Ag transportation and the reduction of Ag^+ to Ag^0.

1. Introduction

2,4-Dichlorophenol (2,4-DCP) is extensively used in many industries such as fungicides, insecticides, pesticides and pharmaceuticals [1], and has been listed as prior pollutants by the U.S. Environmental Protection Agency (EPA) owing to its high toxicity, suspected carcinogenicity, bioaccumulation and mutagenicity to living organisms [2]. 2,4-DCP is abundant in the contaminated groundwater [3], and can cause itch, faint, anemia and comedo [4], provoke disturbances in the structure of cellular bilayer phospholipids [5], pose a serious ecological problem, and seriously affect both public health and environmental quality.

Nanomaterials of noble metals have drawn considerable attention due to their specific mechanical, electrical, optical and catalytic properties compared to their bulk materials [6]. Silver nanoparticles (AgNPs) have been used for many applications in consumer products including textiles, disinfecting medical devices and home appliances, as well as their potential capability of water treatment [7,8]. Considerable interest has arisen in the use of AgNPs for point-of-use systems for emergency response following disasters, and for water systems that are not connected to a central network, owing to the potent and broad-spectrum antimicrobial properties of AgNPs [9,10]. However, with the significant increase in production, application, and market request of AgNPs, it is inevitable for the release of AgNPs into the environment (with the predicted environmental concentration of tens and perhaps hundreds ng/L in water) [11], affecting the normal wastewater processing. According to EPA and World Health Organization, the maximum admissible concentration of silver in drinking water is regulated at 0.1 mg/L.

Furthermore, AgNPs have been reported to be toxic both to humans and the environment [12–15]; and their fate, transport and toxicity can be influenced by water chemistry properties. In turn, the special characteristics of AgNPs will affect the removal of toxic organic pollutants and impact on microbial growth during the process of sewage treatment in the presence of AgNPs in the wastewater.

Researchers have shown that AgNPs can be implicated as efficient catalysts for removal of environmental contaminants, including 4-nitrophenol [16], pentachlorophenol [17], dyes [18], and aromatic nitro compounds [19]. The current reports are mostly concerned with the removal of 2,4-DCP using Ni/Fe [20], Pb/Fe [3], Fe_3O_4 [21], Cu@TiO_2 [22], and other functionalized nanoparticles [23,24], as well as the detection of 2,4-DCP with the nanocomposite acting as a sensor [4]. However, few studies have been reported on the influence of AgNPs on the biodegradation of 2,4-DCP in the wastewater. Among various microorganisms screened, *Phanerochaete chrysosporium* (*P. chrysosporium*), as the model species of white-rot fungi, has been reported to degrade and transform a wide range of organic substrates containing 2,4-DCP in wastewater treatment [25], and, hence, was selected as the testing microorganism in this research.

In order to evaluate the toxicity of AgNPs to *P. chrysosporium* and the effects of AgNPs on the performance of 2,4-DCP biodegradation, dose-response assays of AgNPs, $AgNO_3$ and 2,4-DCP were investigated. Additionally, other factors involved in 2,4-DCP degradation, such as dissolved Ag^+, total Ag (including Ag^+ and AgNPs), pH values, and extracellular proteins content, were also addressed. Based on the analyses of scanning electron microscopy (SEM) equipped with an energy dispersive X-ray (EDX) attachment, Fourier transform infrared spectrometry (FTIR) and gas chromatography–mass spectrometry (GC–MS), toxicity mechanism of AgNPs and the biodegradation pathway of 2,4-DCP were proposed.

2. Materials and methods

2.1. Microorganism and chemicals

P. chrysosporium strain BKMF-1767 (CCTCC AF96007) was obtained from the China Center for Type Culture Collection (Wuhan, China) and maintained on potato dextrose agar slants at 4 °C. Spores suspensions were prepared by scraping the spore into ultrapure water (18.25 MΩ cm), the concentration of which was adjusted to 2.0×10^6 CFU/mL. The cultivation of *P. chrysosporium* was performed in an incubator at 37 °C and 150 rpm for 3 days by inoculating spores suspensions into the culture medium in 500 mL conical flasks. Then, the mycelia were harvested and rinsed several times with 2 mM Na_2HCO_3 buffer solution, which was selected as the exposure medium because it had no effect on silver bioavailability and avoided ligands that might bind with AgNPs/Ag^+ and facilitate precipitation or other confounding effects [26,27].

2,4-DCP and $AgNO_3$ were purchased from Sigma-Aldrich (St. Louis, MO). All other chemicals used were of analytical reagent grade and obtained from Shanghai First Reagent Co., China.

2.2. Characterization of AgNPs

AgNPs were synthesized via reduction of $AgNO_3$ and utilization of $NaBH_4$ and trisodium citrate as reductants and stabilizing agents, respectively, following a protocol adapted from a previous study with minor modifications [28]. Detailed descriptions on preparation and characterization of AgNPs are available in the Supporting information.

2.3. Dose-response assays of AgNPs and $AgNO_3$

The AgNPs stock solution was diluted with 2 mM Na_2HCO_3 buffer solution to obtain the desired concentrations (0, 1, 10, 30, 60, and 100 μM) used in the test solutions and mixed; the initial 2,4-DCP concentration was maintained at 20 mg/L in the flasks. Equivalent fungal mycelia (0.6 g/L) were added to the solutions and incubated in an incubator at 37 °C with 150 rpm. Dose-response assays of $AgNO_3$ were performed similarly.

2.4. Dose-response assay of 2,4-DCP

In order to determine the effect of 2,4-DCP concentration on the adsorption and degradation performance, 0.6 g/L *P. chrysosporium* pellets were exposed to aqueous solutions containing 0, 5, 10, 20, 40, and 80 mg/L 2,4-DCP, respectively, and maintaining an initial AgNPs concentration of 10 μM. 2,4-DCP concentration was determined by high performance liquid chromatography (HPLC, Agilent 1100) with a previously reported method [29]. The intermediates

of 2,4-DCP after biodegradation were identified by GCMS-QP2010 Ultra (Shimadzu, Japan) equipped with a RTX-5 capillary column (30 m × 0.25 mm × 0.25 μm) according to the literature [25,30].

2.5. Instrument and analysis

pH value during the experiment was measured using a laboratory pH meter. Extracelluar protein concentration was analyzed with the Coomassie Brilliant Blue method at 595 nm by a UV–vis spectrophotometer. The removal amounts of 2,4-DCP and Ag were calculated by the differences between the initial and final concentrations of 2,4-DCP and AgNPs/$AgNO_3$ in the solutions. Triplicate assays were performed for each treatment and all of the data were analyzed with Origin 9.0 software.

3. Results and discussion

3.1. Characterization of AgNPs

AgNPs synthesized were spherical crystallite with a mean hydrodynamic diameter of 20.2 ± 0.3 nm and a negative zeta-potential of −30.9 ± 2.3 mV (Fig. S1). A detailed characterization is available in the Supporting information.

3.2. Effects of AgNPs on the removal of 2,4-DCP and total Ag

Treatment with different AgNPs concentrations induced a clear dose-dependent efficiency reduction in 2,4-DCP degradation (Fig. 1A), as measured by dose-response assays of AgNPs. The initial concentrations of AgNPs varying from 0 to 60 μM elicited little impact on the high efficiency of 2,4-DCP (>96%); however, a decrease in 2,4-DCP degradation was observed with a further increase of AgNPs concentration (73.38% for 100 μM). It was found that the 2,4-DCP degradation percentage reached up to ~100% in the media containing *P. chrysosporium* without AgNPs, demonstrating that its biological activity was not significantly affected by a low concentration of 2,4-DCP (20 mg/L), consistent with our prior report [25]. Variation in the total Ag content indicated that AgNPs and other forms of Ag in the liquid phase were transferred into the biological phase, which was assumed to be influenced by produced organic acids and cellular proteins involved in the process. When exposed to low concentrations of AgNPs, especially for 1 μM AgNPs (undetectable after 12 h), a substantial increase in removal rates of total Ag was observed in Fig. 1B (96.11%, 99.63%, 94.17% corresponding to initial AgNPs concentrations of 10, 30, and 60 μM, respectively). In contrast, just 37.35% total Ag was removed for the treatment of 100 μM AgNPs.

High AgNPs concentration (100 μM) gave rise to remarkable reduction in removal rates of 2,4-DCP and total Ag, which could be the reason that the cytotoxicity was induced by AgNPs, resulting in inflammation, apoptosis, and cell death [31]. Mechanisms of AgNPs toxicity, such as damage of membrane integrity, cell cycle arrest, reactive oxygen species (ROS) generation, disruption of energy metabolism, and gene transcription, have been proposed to be involved in AgNPs themselves or released Ag^+ [31]. Consequently, 2,4-DCP degradation, uptake and distribution of AgNPs/Ag^+ were influenced for toxic effects of AgNPs.

In addition, the uptake capability of total Ag exhibited a tendency to linear increase from 0.02 to 1.00 mg/g with the increase of AgNPs concentration in the range of 1–60 μM, but for the highest concentration investigated here, the uptake capability began to decrease (Fig. 1C). This increasing trend might be attributed to that higher AgNPs concentrations caused larger driving force to overcome mass transfer resistance between *P. chrysosporium* and the fluid phase, leading to higher collision probability between *P. chrysosporium* and AgNPs/Ag^+, easier penetration of AgNPs/Ag^+

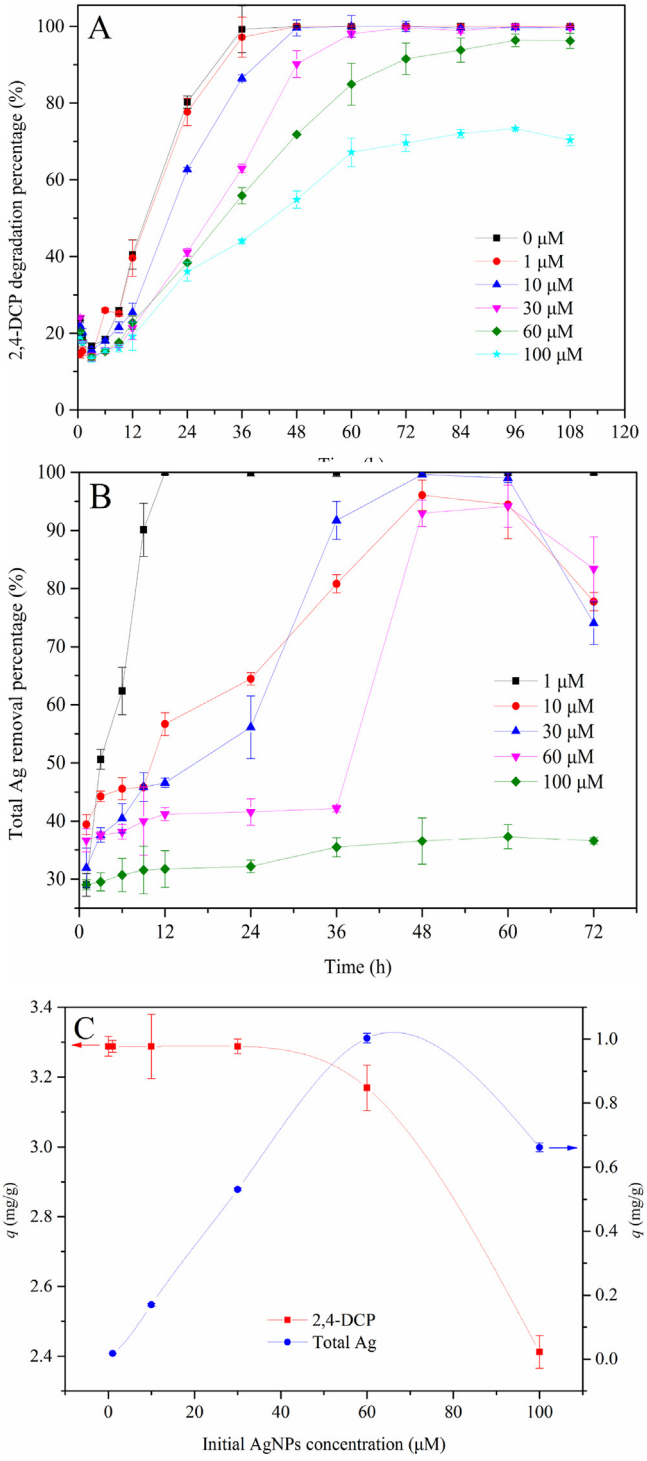

Fig. 1. Effects of AgNPs concentration on the removal of (A) 2,4-DCP and (B) total Ag; (C) were evaluated using the plateau values of the (A) and (B) removal capacities.

to sorption sites, and thus higher uptake of total Ag [25,29]. An excess in AgNPs concentration made some binding sites saturated, further attenuating cellular uptake capability. However, the degradation capacity of 2,4-DCP displayed an equilibrium state and then a sharp decrease with increasing level of AgNPs concentration, which was probably because of the degradation effect of *P. chrysosporium* that was inhibited by high concentrations of AgNPs.

Taken together, these data indicated that AgNPs induced toxicity in a dosage-dependent manner, namely, greater toxicity after

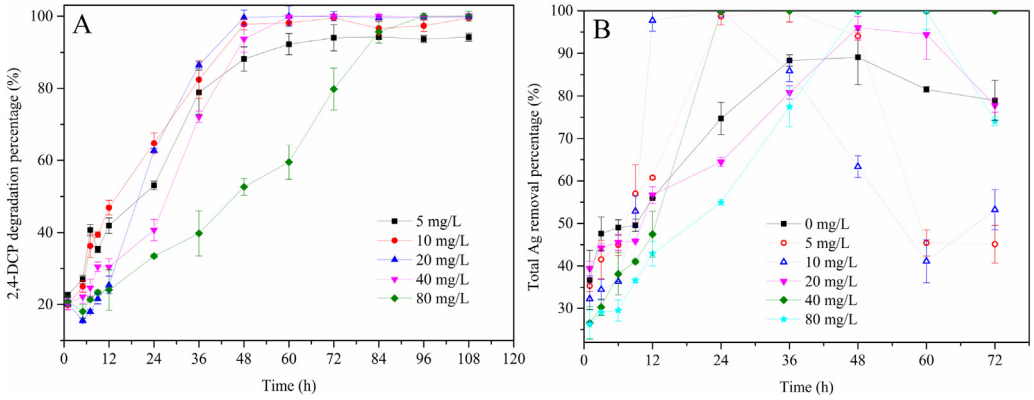

Fig. 2. Effects of 2,4-DCP concentration on the removal of (A) 2,4-DCP and (B) total Ag.

exposure to excessive dosage (100 μM). Moreover, an interesting phenomenon was observed that relatively low concentrations of AgNPs could enhance but not inhibit the biological activity and fitness of microbe, and stimulate the simultaneous removal of 2,4-DCP and total Ag, however, the removal efficacy of which were both decreased under high-dose exposure. The stimulatory effect of AgNPs to the removal of 2,4-DCP and total Ag by *P. chrysosporium* might be the reason that the repair mechanism of *P. chrysosporium* against toxicants was activated under low doses of AgNPs (such as 1–60 μM), leading to overcompensatory for the exposure, which was in tune with the results of earlier studies [27,32,33].

3.3. *Effects of 2,4-DCP on the removal of 2,4-DCP and total Ag*

As the concentration of 2,4-DCP increased from 5 to 40 mg/L, the maximum 2,4-DCP degradation rate increased from 94.21% to ~100%; even for the highest concentration of 80 mg/L, a relatively slow increase to ~100% was still observed (Fig. 2A). It suggested that lower concentrations of 2,4-DCP could be used as carbon and energy sources by *P. chrysosporium* to enhance its biological activity [25,29], further boosting 2,4-DCP degradation, and that high 2,4-DCP concentrations had adverse effects on cells to some extent, but without causing them death completely.

Likewise, the maximum removal rates of total Ag reached approximately 100% for all groups of 2,4-DCP treatment, especially for the treatment of 40 mg/L 2,4-DCP, the total Ag content of which was at undetectable levels after 24 h (Fig. 2B). Maximum removal rates of total Ag achieved much earlier for lower 2,4-DCP concentrations, with two exceptions. One was that without addition of 2,4-DCP, presumably due to lack of organic acids produced during the degradation process of 2,4-DCP to bind to more Ag in comparison to the groups challenged with 2,4-DCP. The other one was the group treated with 20 mg/L 2,4-DCP, presenting a similar trend to that with a concentration of 80 mg/L, which might be the similar chemical properties of both aqueous solutions, such as pH. In addition, it was strange that the uptake rates of total Ag underwent a decline after equilibrium, possibly linked to relative levels of organic acid-bound Ag. Heavy metals complexation with humic acid (a typical organic acid) can regulate metal concentration in aqueous systems, and the dissolution of organic matter was promoted by higher pH [34]. In other words, higher pH could disrupt the complexation between heavy metals and organic acid, resulting in the transport of partial heavy metals into the solution phase again. To validate these hypotheses, changes in pH value of solutions were monitored (Fig. 3).

In the current study, pH was indeed one of the most important parameters affecting the uptake of total Ag in biological settings. When pH level was below 6.94, the corresponding removal rates were >70%; however, a relatively poor removal of total Ag was obtained when pH level was above the range. It is well-known that aqueous metal speciation changed with pH, affecting metal distribution among biological phases by altering their weak interactions such as hydrogen bonds, van der Waals interactions, etc. An elevated pH value adversely influenced the stability of the biomacromolecules and organic acids complexing with metals, thereby decreasing the removal rate of total Ag. It was also found that the pH values of solutions declined initially and subsequently rose over time (Fig. 3). The decline was presumably related to the production of organic acids such as oxalic acid during the process of fungal metabolism and 2,4-DCP degradation [25]; however, the increased pH values demonstrated that organic acids could be consumed as carbon and energy sources at a rate faster than the rate of being produced. Comparing the group only treated with AgNPs with control, the metabolism of *P. chrysosporium* was strongly affected by the transport and fate of AgNPs, which was possibly bound to

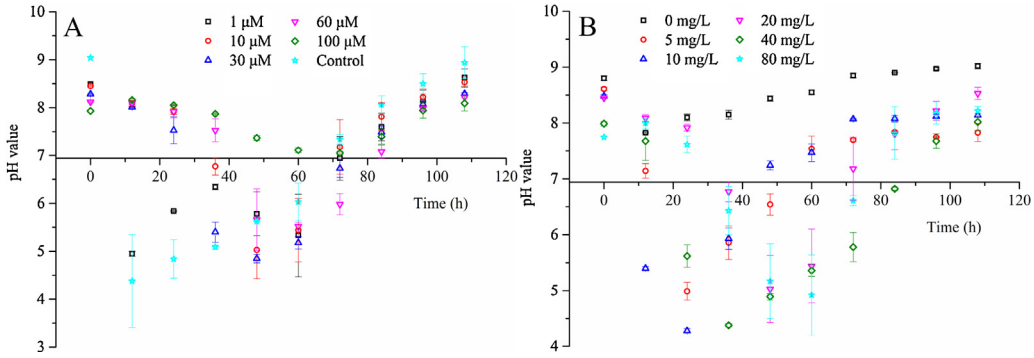

Fig. 3. Changes of pH value after treatment with varying concentrations of (A) AgNPs and (B) 2,4-DCP.

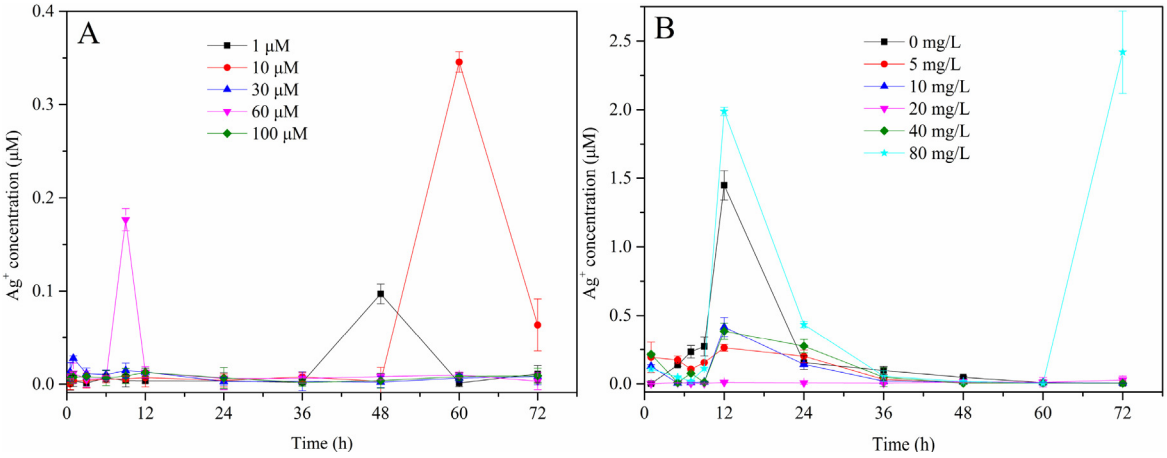

Fig. 4. Concentrations of Ag^+ in the solutions after exposure to different concentrations of (A) AgNPs and (B) 2,4-DCP.

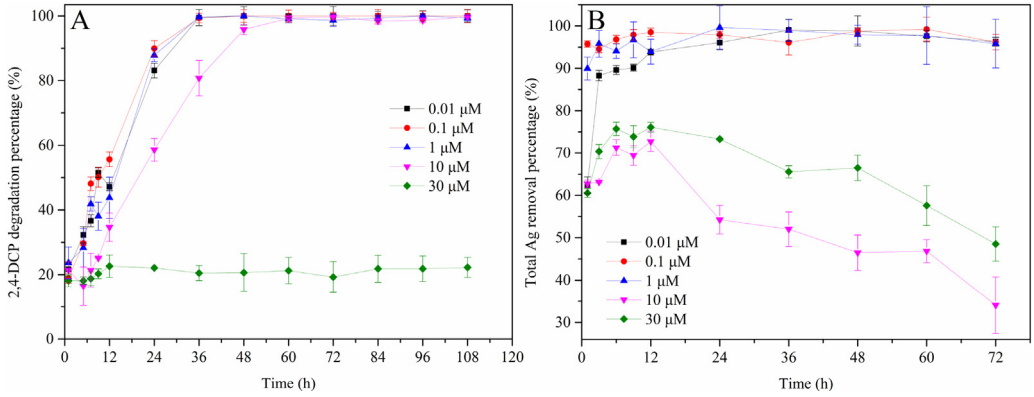

Fig. 5. Effects of $AgNO_3$ concentration on the removal of (A) 2,4-DCP and (B) total Ag.

some kinds of organic acids secreted by white-rot fungi, hence varying the pH of the medium.

3.4. Oxidative dissolution of AgNPs

As is well-known, the release of Ag^+ is of great importance in the transformation of AgNPs in aquatic environments, the process of which has been proposed through oxidizing the nanoparticles in aqueous solutions exposed to air (Equation (1)) and acidic conditions (Equation (2)).

$$4Ag^0 + O_2 \rightarrow 2Ag_2O \quad (1)$$

$$2Ag_2O + 4H^+ \rightarrow 4Ag^+ + 2H_2O \quad (2)$$

Difference and high variability in the release pattern of Ag^+ were observed in the presence of *P. chrysosporium*, the metabolic state of which had an impact on the dissolved oxygen (DO) concentrations, pH values of the solutions and the production of secretions, and removed surface coating materials of AgNPs, enhancing the AgNPs dissolution gradient by binding the released Ag^+ [27,33]. DO in the biological system was sufficient and provided by means of cultivation under 150 rpm. Besides, the dissolution of AgNPs was reported to be enhanced at low pH [14,28]. In this research, low pH values contributed to the release of Ag^+ to some extent. Conversely, when pH values increased, released Ag^+ content was declined in aquatic systems at lower concentrations of 2,4-DCP (Figs. 3B and 4B).

AgNPs with lower initial concentrations tended to slightly aggregate, bringing about more surface areas available for dissolution, and hence enhanced the speed of Ag^+ being released. High concentrations of dissolved Ag^+ at some point were observed under low initial AgNPs concentrations (1, 10, 60 μM), but Ag^+ release was mostly restrained at low levels (Fig. 4A). Natural organic matter (NOM) has been reported to inhibit Ag^+ release from AgNPs by inducing a charge to the particle surface and enhancing the repulsive force among nanoparticles [35]. And extracelluar proteins secreted by *P. chrysosporium* have an effect similar to that of NOM to AgNPs. That could be also explained by the existence of produced organic acids in consequence of biological metabolism and 2,4-DCP degradation. Some organic acids could adhere to the surface of AgNPs, block the available binding sites, and hinder the continual leaching of AgNPs [28,33]. Herein, dissolved Ag^+ in this system could be adsorbed by fungal mycelia, and likewise interfered with cellular proteins, such as the cystein-rich metallothionein [36] and glutathione *S*-transferase [37], which have proved to detoxify Ag^+ by binding them in silver-sulfur nanocrystals. In addition to the formation of Ag complexes, the sharp decline in the concentration of Ag^+ release was likely related to the reduction reaction of hydroxyl groups in polysaccharides and re-association with the original AgNPs [10].

The majority of studies on AgNPs toxicity have proposed that the released Ag^+ was regarded as the primary contributor; however, the low solubility of AgNPs to the bulk solution (Fig. 4A) suggested that the toxicity to *P. chrysosporium* could primarily derived from particle-specific effects of AgNPs, rather than little released Ag^+, as evidenced by previous studies [12,38]. Another possible explanation was that small AgNPs were actively taken up into cells through endocytosis or macropinocytosis [31], and internalized intracellularly to release relatively high localized concentrations of toxic ions within the small size of cells, damaging cell machinery and

Table 1
Changes in extracellular protein content (μg/mL) at different concentrations of AgNPs.

AgNPs concentration (μM)	1 h	12 h	24 h	36 h	48 h	60 h	72 h
0	71.67	67.63	66.28	65.79	65.39	65.15	65.82
1	73.92	66.63	66.61	64.09	65.66	64.15	63.79
10	71.67	71.87	75.36	71.57	68.78	66.46	68.40
30	73.09	78.58	79.42	64.36	62.60	61.09	64.05
60	73.45	83.39	85.95	81.22	71.76	66.11	67.45
100	75.71	82.94	86.45	83.94	82.05	77.38	79.04
Control	70.59	72.73	67.48	64.87	64.95	63.94	64.28

Table 2
Changes in extracellular protein content (μg/mL) at different concentrations of $AgNO_3$.

$AgNO_3$ concentration (μM)	1 h	12 h	24 h	36 h	48 h	60 h	72 h
0.01	71.03	65.68	66.27	64.29	65.66	69.53	72.85
0.1	72.50	59.65	65.36	64.42	64.49	68.93	71.72
1	71.60	65.61	64.91	63.74	65.22	67.67	68.43
10	70.78	66.82	68.28	68.10	71.56	75.19	76.37
30	70.29	69.79	71.56	68.43	69.63	71.03	77.70

exhibiting a "Trojan-horse" effect of AgNPs [39]. Similar results were acquired for dissolved Ag^+ at various initial concentrations of 2,4-DCP (Fig. 4B). No dramatic variation in Ag^+ concentration was noticed under such conditions except that at concentrations of 0 and 80 mg/L, which were plausibly the reasons that no organic acids derived from 2,4-DCP were utilized to hold back dissolution of AgNPs, as discussed above, and that enzymes activity was considerably impacted by a high concentration of 2,4-DCP [25,29], altering the release or availability of Ag^+, respectively.

3.5. Effects of $AgNO_3$ on the removal of 2,4-DCP and total Ag

Ag^+ toxicity under different $AgNO_3$ concentrations was shown in Fig. 5. Ag^+ exerted differential toxicity at low versus high $AgNO_3$ concentrations. Specifically, 2,4-DCP degradation rates were up to ~100% following 60-h exposure to 0.01, 0.1, 1, and 10 μM $AgNO_3$, compared to 22.62% following 12-h exposure to 30 μM $AgNO_3$ (Fig. 5A); lower concentrations of $AgNO_3$ (0.01, 0.1, and 1 μM) caused the removal of total Ag above 90%, while total Ag removal decreased under higher $AgNO_3$ concentrations (67.78% and 72.41% for 10 and 30 μM, respectively) (Fig. 5B). Herein, mechanisms underlying Ag^+ toxicity were likely to the generation of ROS, inducing oxidative stress, and the inactivation of thiol-containing proteins. Additionally, uptake rates of total Ag reduced over time at high $AgNO_3$ concentrations, speculating that perhaps fungal pellets were undergoing apoptosis due to Ag^+ exposure, evoking part of Ag^+ to seep out of the pellets. Overall, the toxicity was clearly positively correlated to Ag^+ concentration and exposure time.

By comparison with AgNPs at the same Ag concentration, $AgNO_3$ is generally more toxic in biological systems, which could be explained as its complete dissociation, releasing large quantities of free Ag^+ very rapidly compared to a slower release of low levels of ionic Ag by AgNPs [40], as well as its higher uptake potential and bioavailability. A higher propensity of Ag^+ than the negative-charged AgNPs should be assimilated by the negative-charged fungal cell wall. Ag^+ had higher binding affinity to sulfur-containing proteins on the cell membrane and in the cytoplasm to make them inactivated, and could also be bound to phosphate-containing molecules such as DNA to damage cells [26]. Nevertheless, it is rather difficult for Ag ions to transport through the membrane and biological barriers freely [41]. As for AgNPs, the particles have been also documented to be greater capability to translocate within cells and even the nuclei [15], interact with crucial cellular components (such as cell membranes and chromosomes) directly [10], and cause a robust inhibition on RNA transcription through its direct binding to RNA polymerase [42], exhibiting the particle-specific toxicity of AgNPs to some degree. Particulate AgNPs was an important source for the overall toxicity of AgNPs, but could play an indirect role through a "Trojan-horse" pathway [43,44]. When getting into the cytoplasm, AgNPs might be oxidized by intracellular ROS, and subsequently release Ag^+, eventually increasing the intracellular toxicity of AgNPs [45]. From the aforementioned analysis and SEM observation (in section 3.7.2), although the exact toxicity mechanisms were not elucidated, AgNPs could potentially elicit biological impacts on cells by means of the "Trojan-horse" mechanism that performed either particle effects or ion effects, or both together contributing to the overall cytotoxicity, in line with recent findings [42].

3.6. Extracellular protein concentration

Stimulation of extracellular protein secreted by *P. chrysosporium* in 2 mM $NaHCO_3$ buffer solution was confirmed upon exposure to various AgNPs concentrations (Table 1). Extracellular proteins for treatments with higher AgNPs concentrations were more abundantly secreted than those for the control (a flask unexposed to AgNPs and 2,4-DCP) and treatments with lower AgNPs concentrations. The data revealed that extracellular proteins were dominated by AgNPs present in the media and substantially stimulated under high concentrations of AgNPs. Additionally, extracellular protein content decreased with exposure time, which was assumed that these proteins could subsequently be targeted as nitrogen sources by *P. chrysosporium* [29].

A wealth of functional groups, such as hydroxyl, amino and carboxyl groups, existed in the extracellular proteins and may interact with AgNPs via electrostatic repulsion, steric and solvation forces, etc. [46]. It is reported that the inhibition of AgNPs to microbes could be somewhat mitigated by way of the interactions between AgNPs and proteins, triggering alterations of AgNPs properties and further affecting cellular uptake of AgNPs and biological activity. The bound proteins also underwent alterations in structure, function and avidity, which in turn influenced AgNPs' interactions with microbes and other proteins [31].

Concerning changes in protein abundance at different $AgNO_3$ concentrations, similar downward trend was found in the first 36 h, although to a lesser extent. However, an increase in extracellular protein contents was observed after 36 h (Table 2), probably due to the fact that Ag^+ toxicity increased with the exposure time and

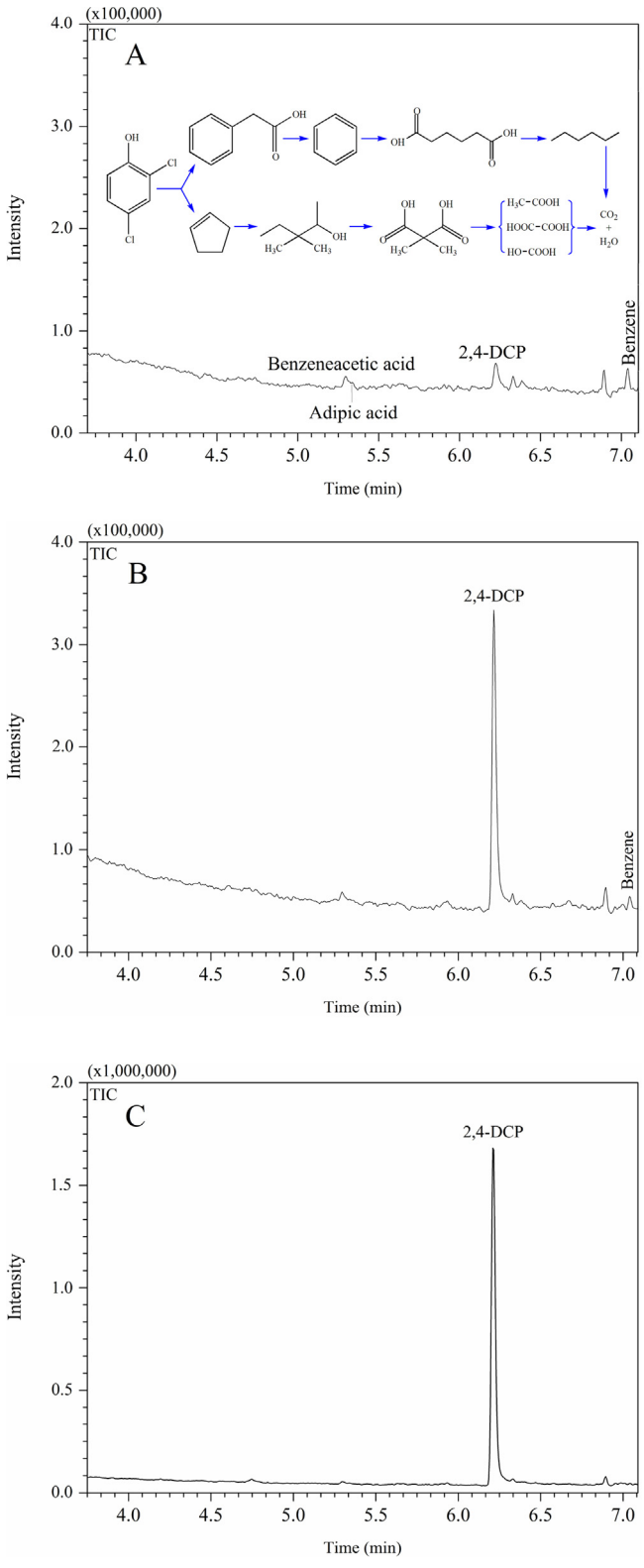

Fig. 6. GC–MS spectra of solutions containing 20 mg/L 2,4-DCP after exposure to (A) 30 μM AgNPs, with its degradation pathways, (B) 100 μM AgNPs, (C) 30 μM $AgNO_3$.

evoked greater production of extracellular proteins to protect the cells from damage. That can be further validated by observations of Fig. 5B and SEM analyses of Fig. 7C, to some degree. Taken together, the excretion of extracellular proteins could be related to Ag^+ and AgNPs, or Ag complexes.

3.7. Mechanism exploration for the removal of 2,4-DCP and total Ag

3.7.1. GC–MS analysis

To confirm the degradation intermediates of 2,4-DCP and conjecture its degradation pathways under different conditions, *P. chrysosporium* was exposed to the solutions with 30 and 100 μM AgNPs, and 30 μM $AgNO_3$ at the same initial 2,4-DCP concentration of 20 mg/L for 60 h. Several intermediates, including benzeneacetic acid, benzene, and adipic acid were clearly detected after exposure to 30 μM AgNPs with the aid of GC–MS (Fig. 6A). Furthermore, some other trace substances were also observed, such as hexane, 3,3-dimethyl-2-pentanol, dimethylmalonic acid, acetic acid, oxalic acid, and carbon acid. Based on the intermediates identified, the underlying degradation pathways were listed in Fig. 6A. Reductive dechlorination of 2,4-DCP occurred first and then the benzene rings were broken down into linear chain organics. Hydroxyl radicals induced by AgNPs via Fenton-like processes under acidic conditions [47] might be another reason for the degradation of chlorophenols, which were decomposed into low-molecule organics and eventually turned into CO_2 and H_2O. In contrast, for the treatments with 100 μM AgNPs and 30 μM $AgNO_3$, the degradation of 2,4-DCP was less apparent because of their potent toxicity to *P. chrysosporium* (Figs. 6B and C), which was consistent with the aforementioned results in Figs. 1A and 5A.

3.7.2. SEM-EDX analysis

For better understanding of the effects of AgNPs and Ag^+ on morphological structure of fungus, SEM measurements on the surface of control, AgNPs-treated and $AgNO_3$-treated fungi were carried out (Fig. 7). The SEM image of control exhibited a network surface structure with smooth hyphae and void spaces between the mycelia (Fig. 7A). The analysis of AgNPs treatment displayed an image of widened mycelia loaded with some crystal particles (Fig. 7B); whereas the outer structure of $AgNO_3$-treated fungus showed the matted mycelia with dense deposits of extracellular secretions, such as extracellular proteins, overlaying the inter-mycelial spaces (Fig. 7C), and, inside of the pellet, vague and compact mycelia were displayed in Fig. 7D. It likely reflected that AgNPs were bound to the mycelial surfaces and that partial AgNPs possibly crossed the cell membrane to exert toxic effects directly or indirectly by releasing Ag^+ owing to oxidative dissolution of AgNPs. However, Ag^+ was left with a significant accumulation on the mycelium due to the membrane barriers. In comparison with the two pellets' EDX spectra (Fig. 7E and F), a clearer Ag peak was observed in the $AgNO_3$-treated spectrum of filamentous interior, revealing that Ag^+ had a more pronounced effect on cell structures with more damage than AgNPs. The reason for the difference is likely that *P. chrysosporium* is more sensitive to Ag^+ than to AgNPs.

3.7.3. FTIR analysis

To gain further insight into the active chemical functional groups responsible for the binding of AgNPs and Ag^+, FTIR was used for analyzing control, AgNPs-treated and $AgNO_3$-treated fungi in the range of 400–4000 cm^{-1}. As shown in Fig. 8, the peak appearing near the region of 3740 cm^{-1} might be the assignment of N—H group, while the peak at 3316 cm^{-1} displayed a strong broad O—H stretching vibration of carboxyl groups superimposed to the N—H stretching band. After challenged with AgNPs and $AgNO_3$, the band was shifted to 3300 cm^{-1}, indicating that carboxyl and N—H groups provided binding sites for AgNPs and Ag^+, and O—H stretching could be involved in the reduction Ag^+ to Ag^0 [33].

An absorption peak observed at 2924 cm^{-1} might be attributed to the symmetric and asymmetric stretching vibration of $-CH_2$ groups of the hydrocarbons on fungal proteins, whereas the peaks around 2360 and 1739 cm^{-1} indicated the presence of P–H and

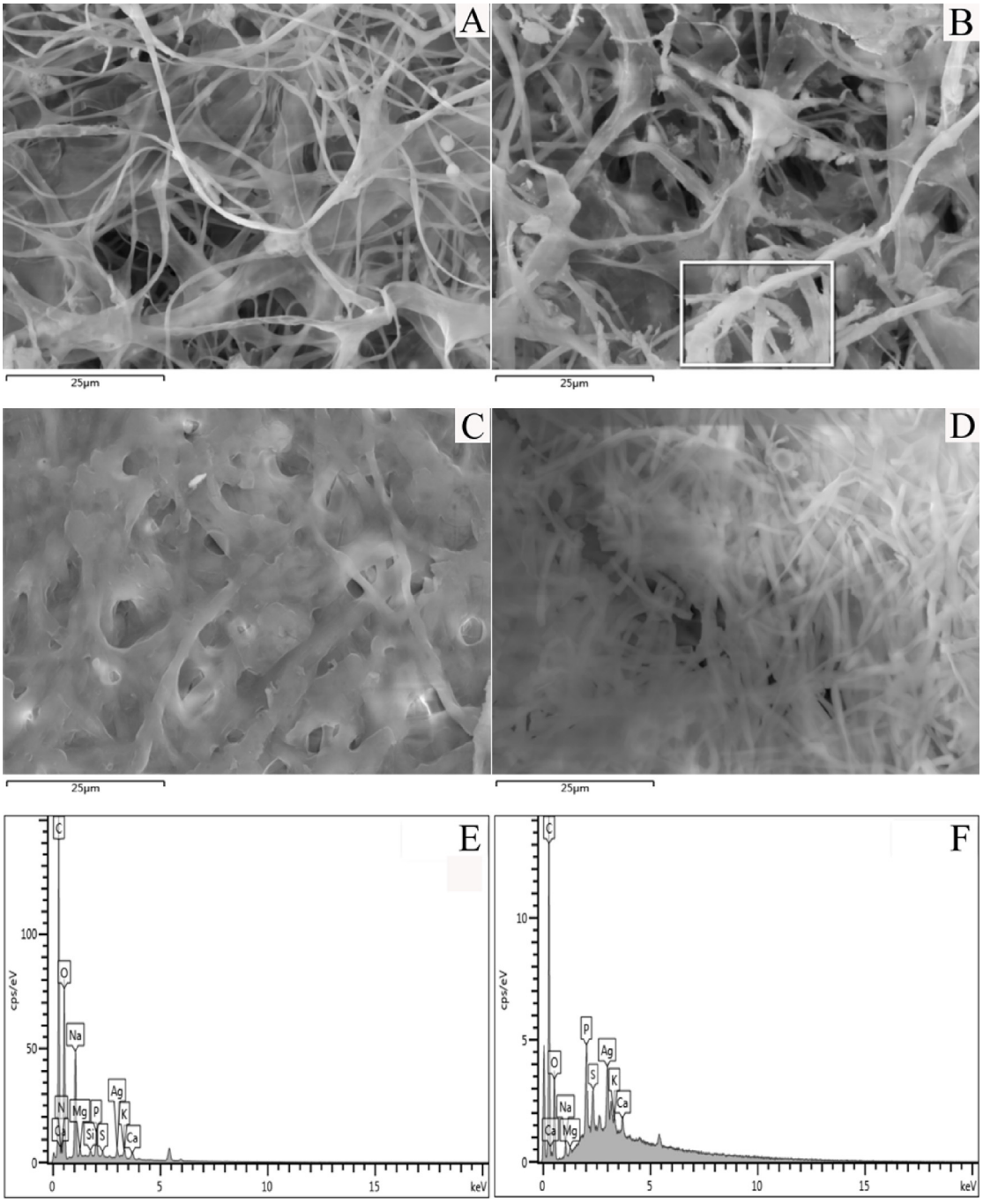

Fig. 7. SEM-EDX micrographs of fungal surfaces: (A) control, (B) with 100 μM AgNPs, and (C) 30 μM $AgNO_3$; (D) SEM and (F) EDX images of fungal pellet interior with 30 μM $AgNO_3$; (E) EDX of denoted area in (B).

carboxyl groups, respectively. Peaks at 1652, 1326 and 1037 cm^{-1} could be assigned to the vibrations of carbonyl (amide I band), C—N stretching from the aromatic and aliphatic amines, respectively. The strengthened intensity of the three bands suggested that the interaction could be possibly performed between AgNPs/Ag^+ and carbonyl group, and conformations of proteins or polypeptides were also affected owing to the binding with AgNPs or reaction with Ag^+. New peaks occurred at 854 and 774 cm^{-1}, representing the deformation vibration of N—H and the asymmetry stretching of P—O—S. The shift from adsorption peak 554–518 cm^{-1} and the disappearance of peak 465 cm^{-1} could be ascribed to P—S and/or P—S—P stretching in cell wall structures. The facts demonstrated that sulfur atoms had potential Ag-binding capacities on the fungus during the reaction. Taken together, functional groups assisting in AgNPs binding were similar to that for Ag^+ even if their spectra were not in complete accord.

4. Conclusions

This report confirmed synergy effects of AgNPs at low doses on 2,4-DCP degradation in the presence of *P. chrysosporium*, where high efficacy of 2,4-DCP degradation (>96%) was obtained. And the removal efficiency of total Ag was maintained at a high level under acidic conditions. By contrast, *P. chrysosporium* was fairly vulnerable to AgNPs at high-level exposure (100 μM) and $AgNO_3$ at relatively low concentrations (10 and 30 μM) due to their overt

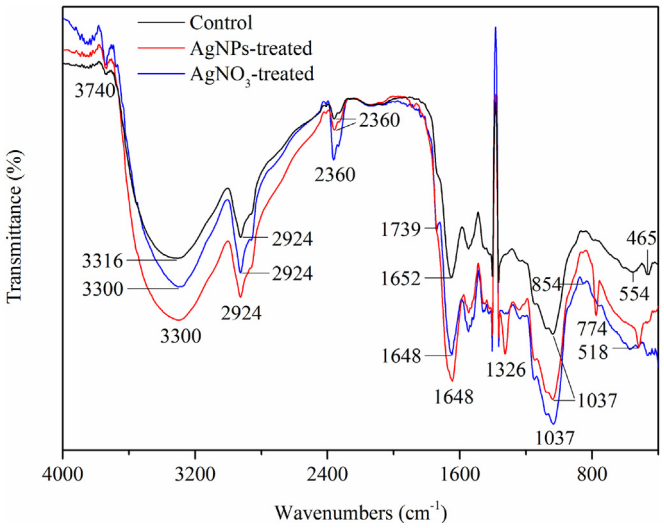

Fig. 8. FTIR spectra of control, AgNPs-treated, and $AgNO_3$-treated fungi.

toxicity with significant suppression on 2,4-DCP degradation and Ag removal. In the current study, the "Trojan-horse" effects of AgNPs could execute particle effects, ion effects, or both inside cells, however, the relative contribution of which needs to be further explored. The mechanisms underlying the complete degradation of 2,4-DCP were involved in reductive dechlorination and reaction with hydroxyl radicals. Ag transportation and the reduction of Ag^+ to Ag^0 were associated with amino, carboxyl, carbonyl, and sulfur-containing groups. These results would subserve the understanding of AgNPs-mediated toxicity and how chlorophenols degradation is regulated by AgNPs, having important implications for AgNPs application in wastewater treatment.

Acknowledgements

This study was financially supported by the National Natural Science Foundation of China (51579099, 51521006 and 51508186), the Program for Changjiang Scholars and Innovative Research Team in University (IRT-13R17), and the Hunan Provincial Innovation Foundation for Postgraduate (CX2016B134).

Appendix A. Supplementary data

Supplementary data associated with this article can be found, in the online version, at http://dx.doi.org/10.1016/j.jhazmat.2016.08.075.

References

[1] J. Xu, X. Lv, J. Li, Y. Li, L. Shen, H. Zhou, X. Xu, Simultaneous adsorption and dechlorination of 2,4-dichlorophenol by Pd/Fe nanoparticles with multi-walled carbon nanotube support, J. Hazard. Mater. 225–226 (2012) 36–45.
[2] Z. Rawajfih, N. Nsour, Characteristics of phenol and chlorinated phenols sorption onto surfactant-modified bentonite, J. Colloid Interface Sci. 298 (2006) 39–49.
[3] Z. Zhang, Q. Shen, N. Cissoko, J. Wo, X. Xu, Catalytic dechlorination of 2,4-dichlorophenol by Pd/Fe bimetallic nanoparticles in the presence of humic acid, J. Hazard. Mater. 182 (2010) 252–258.
[4] X. Wei, Z. Zhou, T. Hao, H. Li, Y. Xu, K. Lu, Y. Wu, J. Dai, J. Pan, Y. Yan, Highly-controllable imprinted polymer nanoshell at the surface of silica nanoparticles based room-temperature phosphorescence probe for detection of 2,4-dichlorophenol, Anal. Chim. Acta 870 (2015) 83–91.
[5] C. Schüller, Y.M. Mamnun, H. Wolfger, N. Rockwell, J. Thorner, K. Kuchler, Membrane-active compounds activate the transcription factors Pdr1 and Pdr3 connecting pleiotropic drug resistance and membrane lipid homeostasis in *Saccharomyces cerevisiae*, Mol. Biol. Cell 18 (2007) 4932–4944.
[6] J. Farkas, P. Christian, J.A.G. Urrea, N. Roos, M. Hassellöv, K.E. Tollefsen, K.V. Thomas, Effects of silver and gold nanoparticles on rainbow trout (*Oncorhynchus mykiss*) hepatocytes, Aquat. Toxicol. 96 (2010) 44–52.
[7] H. Liu, X. Tang, Q. Liu, A novel point-of-use water treatment method by antimicrobial nanosilver textile material, J. Water Health 12 (2014) 670–677.
[8] S.L. Loo, A.G. Fane, T.T. Lim, W.B. Krantz, Y.N. Liang, X. Liu, X. Hu, Superabsorbent cryogels decorated with silver nanoparticles as a novel water technology for point-of-use disinfection, Environ. Sci. Technol. 47 (2013) 9363–9371.
[9] L. Rizzello, P.P. Pompa, Nanosilver-based antibacterial drugs and devices: mechanisms, methodological drawbacks, and guidelines, Chem. Soc. Rev. 43 (2014) 1501–1518.
[10] J.R. Morones, J.L. Elechiguerra, A. Camacho, K. Holt, J.B. Kouri, J.T. Ramírez, M.J. Yacaman, The bactericidal effect of silver nanoparticles, Nanotechnology 16 (2005) 2346–2353.
[11] N.C. Mueller, B. Nowack, Exposure modelling of engineered nanoparticles in the environment, Environ. Sci. Technol. 42 (2008) 4447–4453.
[12] J. Fabrega, S.R. Fawcett, J.C. Renshaw, J.R. Lead, Silver nanoparticle impact on bacterial growth: effect of pH, concentration, and organic matter, Environ. Sci. Technol. 43 (2009) 7285–7290.
[13] J. Fabrega, S.N. Luoma, C.R. Tyler, T.S. Galloway, Silver nanoparticles: behaviour and effects in the aquatic environment, Environ. Int. 37 (2011) 517–531.
[14] C. Levard, E.M. Hotze, G.V. Lowry, G.E. Brown Jr., Environmental transformations of silver nanoparticles: impact on stability and toxicity, Environ. Sci. Technol. 46 (2012) 6900–6914.
[15] P.V. AshaRani, G. Low Kah Mun, M.P. Hande, S. Valiyaveettil, Cytotoxicity and genotoxicity of silver nanoparticles in human cells, ACS Nano 3 (2009) 279–290.
[16] N. Muniyappan, N.S. Nagarajan, Green synthesis of silver nanoparticles with *Dalbergia spinosa* leaves and their applications in biological and catalytic activities, Process Biochem. 49 (2014) 1054–1061.
[17] L. Yu, X. Yang, Y. Ye, X. Peng, D. Wang, Silver nanoparticles decorated anatase TiO_2 nanotubes for removal of pentachlorophenol from water, J. Colloid Interface Sci. 453 (2015) 100–106.
[18] A. Vanaamudan, H. Soni, P.P. Sudhakar, Palm shell extract capped silver nanoparticles—As efficient catalysts for degradation of dyes and as SERS substrates, J. Mol. Liq. 215 (2016) 787–794.
[19] T. Sinha, M. Ahmaruzzaman, A.K. Sil, A. Bhattacharjee, Biomimetic synthesis of silver nanoparticles using the fish scales of Labeo rohita and their application as catalysts for the reduction of aromatic nitro compounds, Spectrochim. Acta Part A 131 (2014) 413–423.
[20] D. Zhao, Y. Zheng, M. Li, S.A. Baig, D. Wu, X. Xu, Catalytic dechlorination of 2,4-dichlorophenol by Ni/Fe nanoparticles prepared in the presence of ultrasonic irradiation, Ultrason. Sonochem. 21 (2014) 1714–1721.
[21] L. Xu, J. Wang, Fenton-like degradation of 2,4-dichlorophenol using Fe_3O_4 magnetic nanoparticles, Appl. Catal. B 123 (2012) 117–126.
[22] Z. Wang, L. Zang, X. Fan, H. Jia, L. Li, W. Deng, C. Wang, Defect-mediated of Cu@TiO_2 core–shell nanoparticles with oxygen vacancies for photocatalytic degradation 2,4-DCP under visible light irradiation, Appl. Surf. Sci. 358 (2015) 479–484.
[23] J. Xu, X. Liu, G.V. Lowry, Z. Cao, H. Zhao, J.L. Zhou, X. Xu, Dechlorination mechanism of 2,4-dichlorophenol by magnetic MWCNTs supported Pd/Fe nanohybrids: rapid adsorption, gradual dechlorination, and desorption of phenol, ACS Appl. Mater. Interfaces 8 (2016) 7333–7342.
[24] J. Wan, J. Wan, Y. Ma, M. Huang, Y. Wang, R. Ren, Reactivity characteristics of SiO_2-coated zero-valent iron nanoparticles for 2,4-dichlorophenol degradation, Chem. Eng. J. 221 (2013) 300–307.
[25] A. Chen, G. Zeng, G. Chen, J. Fan, Z. Zou, H. Li, X. Hu, F. Long, Simultaneous cadmium removal and 2,4-dichlorophenol degradation from aqueous solutions by *Phanerochaete chrysosporium*, Appl. Microbiol. Biotechnol. 91 (2011) 811–821.
[26] Z.M. Xiu, J. Ma, P.J.J. Alvarez, Differential effect of common ligands and molecular oxygen on antimicrobial activity of silver nanoparticles versus silver ions, Environ. Sci. Technol. 45 (2011) 9003–9008.
[27] Z.M. Xiu, Q.B. Zhang, H.L. Puppala, V.L. Colvin, P.J.J. Alvarez, Negligible particle-specific antibacterial activity of silver nanoparticles, Nano Lett. 12 (2012) 4271–4275.
[28] J. Liu, R.H. Hurt, Ion release kinetics and particle persistence in aqueous nano-silver colloids, Environ. Sci. Technol. 44 (2010) 2169–2175.
[29] Z. Huang, G. Chen, G. Zeng, A. Chen, Y. Zuo, Z. Guo, Q. Tan, Z. Song, Q. Niu, Polyvinyl alcohol-immobilized *Phanerochaete chrysosporium* and its application in the bioremediation of composite-polluted wastewater, J. Hazard. Mater. 289 (2015) 174–183.
[30] G. Chen, S. Guan, G. Zeng, X. Li, A. Chen, C. Shang, Y. Zhou, H. Li, J. He, Cadmium removal and 2,4-dichlorophenol degradation by immobilized *Phanerochaete chrysosporium* loaded with nitrogen-doped TiO_2 nanoparticles, Appl. Microbiol. Biotechnol. 97 (2013) 3149–3157.
[31] Z. Wang, T. Xia, S. Liu, Mechanisms of nanosilver-induced toxicological effects: more attention should be paid to its sublethal effects, Nanoscale 7 (2015) 7470–7481.
[32] Z. Guo, G. Chen, L. Liu, G. Zeng, Z. Huang, A. Chen, L. Hu, Activity variation of *Phanerochaete chrysosporium* under nanosilver exposure by controlling of different sulfide sources, Sci. Rep. 6 (2016) 20813–20818.
[33] Y. Zuo, G. Chen, G. Zeng, Z. Li, M. Yan, A. Chen, Z. Guo, Z. Huang, Q. Tan, Transport fate, and stimulating impact of silver nanoparticles on the removal

of Cd(II) by *Phanerochaete chrysosporium* in aqueous solutions, J. Hazard. Mater. 285 (2015) 236–244.
[34] Y. Yin, C.A. Impellitteri, S.J. You, H.E. Allen, The importance of organic matter distribution and extract soil: solution ratio on the desorption of heavy metals from soils, Sci. Total Environ. 287 (2002) 107–119.
[35] Y. Liang, S.A. Bradford, J. Simunek, M. Heggen, H. Vereecken, E. Klumpp, Retention and remobilization of stabilized silver nanoparticles in an undisturbed loamy sand soil, Environ. Sci. Technol. 47 (2013) 12229–12237.
[36] A.B. Lansdown, Critical observations on the neurotoxicity of silver, Crit. Rev. Toxicol. 37 (2007) 237–250.
[37] S. Kristiansen, P. Ifversen, G. Danscher, Ultrastructural localization and chemical binding of silver ions in human organotypic skin cultures, Histochem. Cell Biol. 130 (2008) 177–184.
[38] L. Yin, Y. Cheng, B. Espinasse, B.P. Colman, M. Auffan, M. Wiesner, J. Rose, J. Liu, E.S. Bernhardt, More than the ions: the effects of silver nanoparticles on *Lolium multiflorum*, Environ. Sci. Technol. 45 (2011) 2360–2367.
[39] A.R. Gliga, S. Skoglund, I.O. Wallinder, B. Fadeel, H.L. Karlsson, Size-dependent cytotoxicity of silver nanoparticles in human lung cells: the role of cellular uptake, agglomeration and Ag release, Part. Fibre Toxicol. 11 (2014) 11.
[40] G. Laban, L.F. Nies, R.F. Turco, J.W. Bickham, M.S. Sepúlveda, The effects of silver nanoparticles on fathead minnow (*Pimephales promelas*) embryos, Ecotoxicology 19 (2010) 185–195.
[41] A.M. Studer, L.K. Limbach, L. Van Duc, F. Krumeich, E.K. Athanassiou, L.C. Gerber, H. Moch, W.J. Stark, Nanoparticle cytotoxicity depends on intracellular solubility: comparison of stabilized copper metal and degradable copper oxide nanoparticles, Toxicol. Lett. 197 (2010) 169–174.
[42] Z. Wang, S. Liu, J. Ma, G. Qu, X. Wang, S. Yu, J. He, J. Liu, T. Xia, G.-B. Jiang, Silver nanoparticles induced RNA polymerase-silver binding and RNA transcription inhibition in erythroid progenitor cells, ACS Nano 7 (2013) 4171–4186.
[43] N. Lubick, Nanosilver toxicity: ions: nanoparticles-or both? Environ. Sci. Technol. 42 (2008) 8617.
[44] E.-J. Park, J. Yi, Y. Kim, K. Choi, K. Park, Silver nanoparticles induce cytotoxicity by a Trojan-horse type mechanism, Toxicol. In Vitro 24 (2010) 872–878.
[45] C. Zhang, Z. Hu, B. Deng, Silver nanoparticles in aquatic environments: physiochemical behavior and antimicrobial mechanisms, Water Res. 88 (2016) 403–427.
[46] A.E. Nel, L. Mädler, D. Velegol, T. Xia, E.M.V. Hoek, P. Somasundaran, F. Klaessig, V. Castranova, M. Thompson, Understanding biophysicochemical interactions at the nano–bio interface, Nat. Mater. 8 (2009) 543–557.
[47] D. He, C.J. Miller, T.D. Waite, Fenton-like zero-valent silver nanoparticle-mediated hydroxyl radical production, J. Catal. 317 (2014) 198–205.